JACS Au
AN OPEN ACCESS JOURNAL OF THE AMERICAN CHEMICAL SOCIETY

pubs.acs.org/jacsau

Article

Unraveling the Bonding Complexity of Polyhalogen Anions: High-Pressure Synthesis of Unpredicted Sodium Chlorides Na_2Cl_3 and Na_4Cl_5 and Bromide Na_4Br_5

Yuqing Yin,* Alena Aslandukova, Nityasagar Jena, Florian Trybel, Igor A. Abrikosov, Bjoern Winkler, Saiana Khandarkhaeva, Timofey Fedotenko, Elena Bykova, Dominique Laniel, Maxim Bykov, Andrey Aslandukov, Fariia I. Akbar, Konstantin Glazyrin, Gaston Garbarino, Carlotta Giacobbe, Eleanor L. Bright, Zhitai Jia, Leonid Dubrovinsky, and Natalia Dubrovinskaia

Cite This: *JACS Au* 2023, 3, 1634−1641

Read Online

ACCESS | Metrics & More | Article Recommendations | Supporting Information

ABSTRACT: The field of polyhalogen chemistry, specifically polyhalogen anions (polyhalides), is rapidly evolving. Here, we present the synthesis of three sodium halides with unpredicted chemical compositions and structures (*tP*10-Na_2Cl_3, *hP*18-Na_4Cl_5, and *hP*18-Na_4Br_5), a series of isostructural cubic *cP*8-AX_3 halides ($NaCl_3$, KCl_3, $NaBr_3$, and KBr_3), and a trigonal potassium chloride (*hP*24-KCl_3). The high-pressure syntheses were realized at 41−80 GPa in diamond anvil cells laser-heated at about 2000 K. Single-crystal synchrotron X-ray diffraction (XRD) provided the first accurate structural data for the symmetric trichloride Cl_3^- anion in *hP*24-KCl_3 and revealed the existence of two different types of infinite linear polyhalogen chains, $[Cl]_\infty^{n-}$ and $[Br]_\infty^{n-}$, in the structures of *cP*8-AX_3 compounds and in *hP*18-Na_4Cl_5 and *hP*18-Na_4Br_5. In Na_4Cl_5 and Na_4Br_5, we found unusually short, likely pressure-stabilized, contacts between sodium cations. Ab initio calculations support the analysis of structures, bonding, and properties of the studied halogenides.

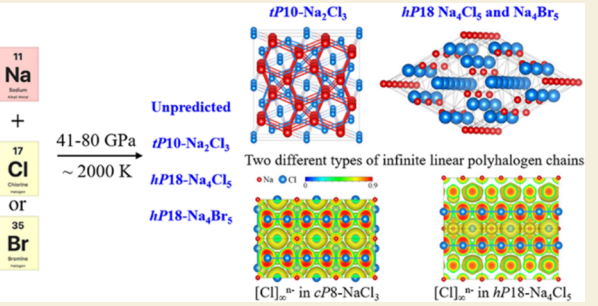

KEYWORDS: *halogen bonding, polyhalogen anions, alkali halides, high-pressure chemistry, X-ray diffraction*

1. INTRODUCTION

High pressure (HP) dramatically changes the chemistry of materials.[1] Quantum-chemical calculations predict unusual but stable stoichiometries of alkali halides, such as, for example, $NaCl_3$ and $NaCl_7$,[2] Na_2Cl, Na_3Cl_2, and Na_4Cl_3,[2,3] Li_nI (n = 2−5),[4] and CsF_m (m = 2−6),[5,6] and suggest uncommon properties. Despite the numerous predictions, very few of them have been experimentally confirmed.

So far, the syntheses of the compounds with the stoichiometries AX_3, A_3X, and AX_5 (A is an alkali metal, and X is a halogen) have been reported at high pressures. The list includes, for example, polymorphs of $NaCl_3$ (space groups *Pnma* and $Pm\bar{3}n$),[2] KCl_3 ($Pm\bar{3}n$ and $P\bar{3}c1$),[7] KBr_3 (*Pnma* and $P\bar{3}c1$),[8] CsI_3 (*Pnma*, $P\bar{3}c1$, and $Pm\bar{3}n$),[9,10] and Na_3Cl ($P4/mmm$)[2] and KBr_5 ($P2_1$)[8] compounds. The majority of them were characterized in a diamond anvil cell (DAC) using powder X-ray diffraction (XRD) and Le Bail analysis, and only the two polymorphs of CsI_3 (*Pnma* and $P\bar{3}c1$)[10] were studied using single-crystal XRD (SCXRD). Although the synergy of powder XRD and ab initio structure predictions is very helpful to obtain a structure solution, the interpretation of some powder XRD remains ambiguous (e.g., those of KBr_3 and KBr_5).[8]

SCXRD provides both a precise structure determination and the chemical composition of the products of reactions in a laser-heated DAC (LHDAC) and has become the ultimate method of HP chemical crystallography.[11−14] In this work, using SCXRD on samples in LHDACs, we have studied chemical reactions in the four A−X systems (Na−Cl, Na−Br, K−Cl, and K−Br) at different pressures (see Table S1). As a result, a number of *cP*8-AX_3 isostructural cubic ($Pm\bar{3}n$) compounds ($NaCl_3$, KCl_3, $NaBr_3$, and KBr_3) and a trigonal ($P\bar{3}c1$) *hP*24-KCl_3 were synthesized; their structures were solved and refined. Sodium and potassium tribromides were previously unknown. New polyhalides of sodium, Na_4Cl_5 and Na_4Br_5, and a sodium sesquichloride, Na_2Cl_3, with hitherto unpredicted compositions and structures, were obtained and fully characterized using SCXRD. Our ab initio calculations

Received: February 21, 2023
Revised: May 10, 2023
Accepted: May 11, 2023
Published: June 5, 2023

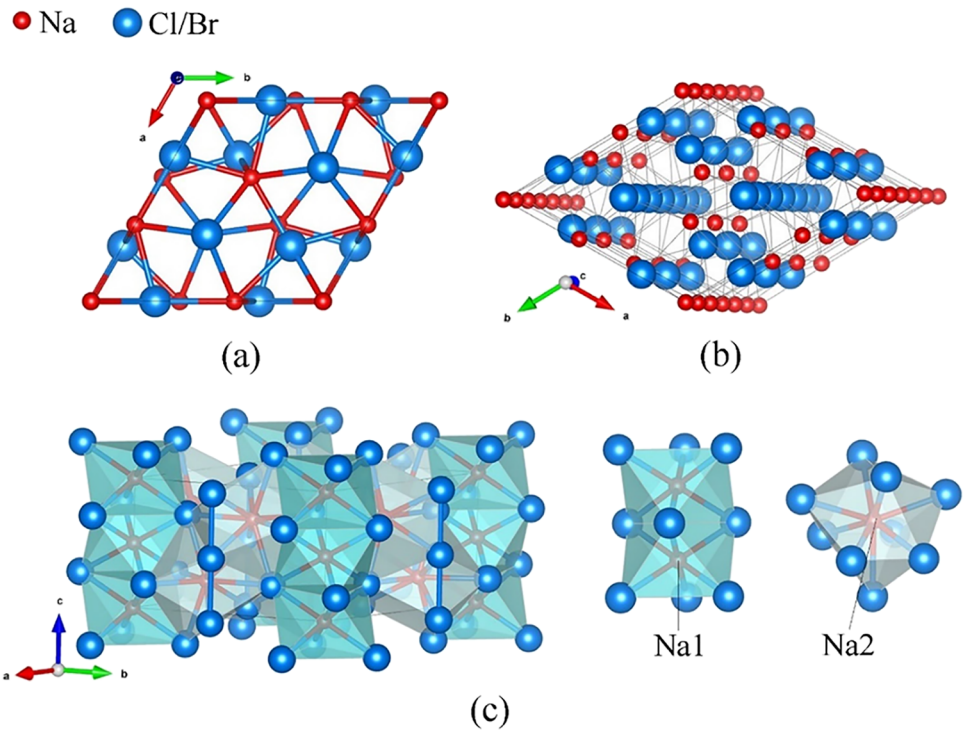

Figure 1. Structure of the novel isostructural sodium polychloride $hP18$-Na_4Cl_5 and sodium polybromide $hP18$-Na_4Br_5 synthesized in this work. (a) Unit cell viewed along the c direction; Na atoms are red, and Cl (or Br) atoms are blue; (b) perspective view of the structure highlighting the linear polyhalogen chains along the c direction; and (c) polyhedral model of the structure; coordination polyhedra for Na1 and Na2 atoms are shown separately.

reveal electronic properties and chemical bonding in novel compounds.

2. EXPERIMENTAL METHOD

Experiments have been performed in the pressure range of 41−80 GPa (for details see Supplementary Methods). As starting materials, high-purity, well-dried NaCl, NaBr, and KBr were used. A chosen alkali halide was loaded into a DAC along with either liquid carbon tetrachloride (CCl_4) or solid carbon tetrabromide (CBr_4), which decompose under laser heating above 40 GPa[15−17] and serve as sources of the halogen atoms. As far as carbon from diamond anvils is unavoidably present in the pressure chamber,[18] carbon-containing CCl_4 and CBr_4 do not introduce extra contamination of the system. The samples were compressed to the target pressures and laser-heated. Then SCXRD was collected in situ at room temperature. A summary of all LHDAC experiments is provided in Table S1.

3. RESULTS AND DISCUSSION

3.1. Observation of the AX_3 Compounds

The formation of $cP8$-AX_3 isostructural halides (Pearson symbol $cP8$; space group $Pm\bar{3}n$, #223), $NaCl_3$, KCl_3, KBr_3, and $NaBr_{3-x}$, was observed in the corresponding A−X systems. Their structures were solved and refined; full crystallographic data and refinement details are provided in Tables S2−S6. Na (or K) occupies the 2a Wyckoff position (000) in the nodes of the bcc lattice. Cl (or Br) atoms in the 6d Wyckoff position (1/4 1/2 0) form linear chains (Figure S1a). $cP8$-KBr_3 and $cP8$-$NaBr_{3-x}$ were experimentally observed for the first time. According to the structure refinement, the occupancy of the Br1 atomic position in $cP8$-$NaBr_{3-x}$ is partial and equal to 0.72(8) and 0.757(17) at 46 and 73 GPa, respectively. The refinement of the structure model with the full occupancy of the Br1 atomic position results in larger values of the agreement factors (R_1) (Table S6). A Hamilton significance test[19] allowed us to judge that the improvement of the agreement factors for the model with the partial occupancy may be considered significant. According to the Hamilton test, the structure model with the partial occupancy of the Br1 atomic position is preferable with the 90−95% confidence level at 46 GPa and more than 99.5% at 73 GPa. The results of our density functional theory (DFT) calculations show that the parameters of the DFT-relaxed structures agree well with the experimental data (Tables S2−S5).

In the K−Cl system, we observed not only a cubic but also a trigonal polymorph of KCl_3 ($hP24$, $P\bar{3}c1$, #165) (see Table S7 for full crystallographic data). Its structure was previously known,[7] but we refined it based on SCXRD analysis (Table S7 and Figure S1b). It consists of rows of potassium atoms oriented along the c direction and isolated linear $[Cl_3]^-$ ions. The appearance of $hP24$-KCl_3 after a chemical reaction in the sample ($KCl + CCl_4 + C_{graphite}$), pressurized in DAC #2 to 41 GPa, and then laser-heated, was especially remarkable. Before heating, the sample looked gray and translucent (due to graphite used as a laser light absorber), but after laser heating, it turned red and transparent (Figure S2a, left). Upon further compression to 50 GPa, the color became much darker (Figure S2b, left) that can be explained by the decreasing of the band gap of the $hP24$-KCl_3 semiconductor material as revealed by our ab initio calculations (Figure S2a,b, right). For $hP24$-KCl_3 and all $cP8$-AX_3 compounds ($cP8$-$NaCl_3$, $cP8$-KCl_3, and $cP8$-KBr_3), our experimental data on the pressure dependence of the volume per atom (V_0/atom) fit well with the results of our DFT calculations (Figure S3a,b).

https://doi.org/10.1021/jacsau.3c00090
JACS Au 2023, 3, 1634−1641

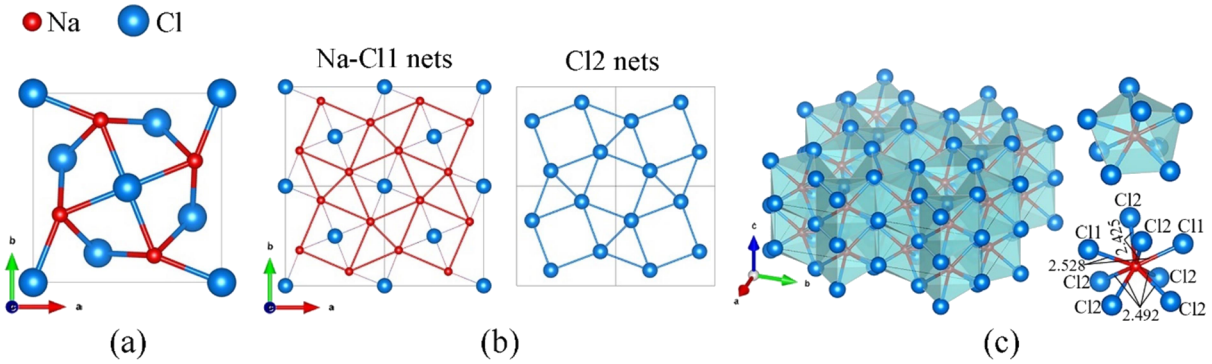

Figure 2. Structure of the novel sodium sesquichloride $tP10$-Na_2Cl_3 synthesized in this work. (a) Unit cell viewed along the c direction; Na atoms are red, and Cl atoms are blue; (b) Na−Cl1 nets and Cl2 nets, which alternate in the c direction (Na and Cl2 form the 2D tiling of the same $3^2.4.3.4$ topology); and (c) polyhedral model of the structure; the Na coordination polyhedron is shown separately.

3.2. High-Pressure Synthesis of Na_2Cl_3, Na_4Cl_5, and Na_4Br_5: Crystal Structures, Stability, and Raman Spectra

SCXRD analysis using the DAFi program[12] revealed three other sodium chlorine and sodium bromine compounds which have never been predicted from ab initio calculations: the isostructural $hP18$-Na_4Cl_5 and $hP18$-Na_4Br_5 (space group $P6_3/mcm$, #193) and $tP10$-Na_2Cl_3 (space group $P4/mbm$, #127) (see Tables S8−S10 for crystallographic details). Their chemical formulas resulted from a structure solution and refinement.

The $hP18$-Na_4Cl_5 compound was first synthesized at 50 GPa and 2100 K. At 50 GPa, it has the following lattice parameters: a = 7.329(2) Å and c = 4.776(18) Å. In its crystal structure (see Figure 1 and Table S8, and the CIF deposited at CSD 2224055), Na1 and Na2 are in the 2b and 6g Wyckoff sites, and Cl1 and Cl2 are in 4d and 6g, respectively. Cl1 atoms form linear chains aligned along the c direction with the Cl1−Cl1 distance of 2.3879(9) Å. Na1 atoms also form linear chains aligned along the c direction with the Na1−Na1 distance of 2.3879(9) Å (Figure 1b). Na1 atoms are coordinated by six Cl2 atoms forming an octahedron with an edge length of 3.1314(17) Å. The face-sharing $Na1Cl2_6$ octahedra form columns in the polyhedral model of the $hP18$-Na_4Cl_5 structure (Figure 1c). Na2 is coordinated by both the Cl1 and Cl2 atoms with the coordination number CN = 9, forming $Na2Cl_9$ polyhedra (distorted capped square antiprisms) filling the space between the columns of the face-sharing $Na1Cl2_6$ octahedra (Figure 1c).

$hP18$-Na_4Br_5, observed at 48 and 73 GPa (see Table S1), was found to be isostructural to $hP18$-Na_4Cl_5. For crystallographic details, see Table S9 and the CIF deposited at CSD 2224057.

The chemical reaction of NaCl with CCl_4 in DAC #1 (Table S1) at 50 GPa and 2100 K led to the formation of numerous good-quality single-crystal domains, which were identified as a sesquichloride of sodium, $tP10$-Na_2Cl_3 (space group $P4/mbm$, #127), also observed at 56 GPa (see Tables S1 and S10 and the CIF deposited at CSD 2224059). This compound has not been observed or predicted so far. In the crystal structure of $tP10$-Na_2Cl_3 (Figure 2), Na atoms occupy the 4g Wyckoff site, and Cl1 and Cl2—the 2a and 4h sites, respectively. Its lattice parameters at 50(1) GPa are a = 6.569(2) Å and c = 3.076(16) Å. The unit cell, as viewed along the c direction, is shown in Figure 2a. The structure can be easily visualized as an alternation of Na−Cl1 and Cl2 nets along the c direction (Figure 2b). In the Na−Cl1 nets, Cl1 atoms are located in the centers of squares of the $3^2.4.3.4$ 2D tiling formed by Na atoms in the ab plane (Figure 2b, left), which has the same topology as Cl2 nets (Figure 2b, right). For a polyhedral presentation, one should consider that Na has the CN = 8 with respect to Cl atoms forming a distorted square antiprism (Figure 2c) with an average Na−Cl distance of 2.484(3) Å. These antiprisms belong to the class of hendecahedrons (polyhedra with 11 faces) which, by sharing common faces, make a 3D tiling of the whole space (Figure 2c). The structure of $tP10$-Na_2Cl_3 can be viewed as "inverse" of that predicted for Na_3Cl_2[2] if sodium and chlorine would swap their positions.

Our DFT calculations reproduced the crystal structures of $hP18$-Na_4X_5 (X = Cl or Br) and $tP10$-Na_2Cl_3 (Tables S8−S10). The pressure dependences of the volume per atom for these compounds (based on the pressure−volume relations from our DFT calculations), in comparison with experimental data, are shown in Figure S3c,d. The parameters of the third-order Birch−Murnaghan (BM3) equations of states (EOSes) are provided in Table S11. Our DFT results confirmed the dynamical stability of $hP18$-Na_4Cl_5 and $hP18$-Na_4Br_5 above 10 and 30 GPa, respectively (Figure S4), and indicated their thermodynamic stability on the convex hull diagram (see Figure 3 for $hP18$-Na_4Cl_5 and Figure S5 for $hP18$-Na_4Br_5).

Considering the stability of $tP10$-Na_2Cl_3, we have found that at its synthesis pressure of about 50 GPa, the corresponding point is located 111 meV/atom above the static convex hull simulated at 0 K (Figure 3a). Harmonic phonon dispersion calculated at 50 GPa shows imaginary modes (Figure S6a), which contradicts our experimental observations. The finite-temperature calculations of phonon dispersion relations at T = 300 K and at P = 50 GPa, including thermal and anharmonic effects, are found to weaken the instability (see Figure S6b) though it does not remove it completely. Increasing the pressure further stabilizes $tP10$-Na_2Cl_3: in calculations carried out at 100 GPa, the phase is dynamically stable in the harmonic approximation already at T = 0 K (Figure S6c). The disagreement between theoretical calculations and experiment on the pressure at which $tP10$-Na_2Cl_3 is stabilized might be due to limitations of DFT calculations and require further studies. However, it does not influence the principal conclusions of this work and would be reported elsewhere.

Figure S7 shows the Raman spectrum taken from the sample in DAC #1 at 50 GPa and room temperature after a NaCl + CCl_4 + $C_{graphite}$ mixture was laser heated to ∼2000 K. The spatial distribution of the reaction products, which were formed upon heating, was determined using XRD mapping of

https://doi.org/10.1021/jacsau.3c00090
JACS Au 2023, 3, 1634−1641

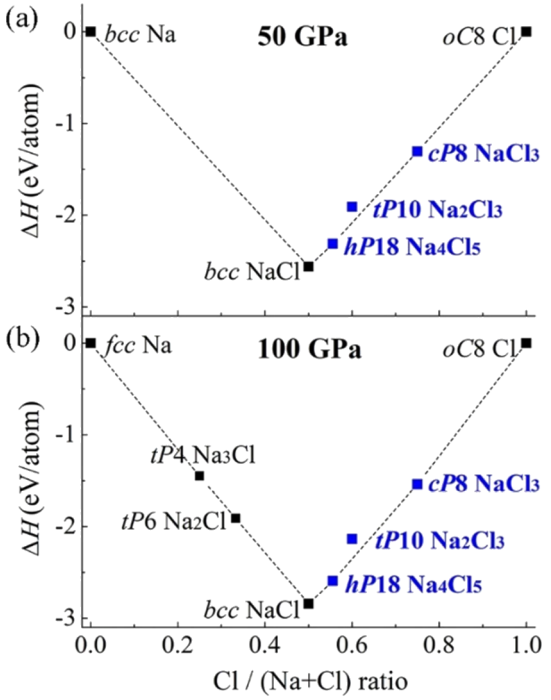

Figure 3. Convex hull diagrams for the Na−Cl system at different pressures. (a) 50 GPa; (b) 100 GPa. The compounds synthesized in this work are highlighted in blue bold font.

the whole sample chamber. It revealed an uneven distribution of B2-NaCl, *h*P18-Na_4Cl_5, *t*P10-Na_2Cl_3, and *c*P8-$NaCl_3$ phases formed in DAC #1. We calculated the positions of the Brillouin-zone-center optical phonons for *c*P8-$NaCl_3$ and *h*P18-Na_4Cl_5 and could conclude that all phases might contribute to the Raman spectrum we observed. The Raman peak at 323 cm^{-1} (marked with an asterisk in Figure S7) can be assigned to the A_g mode of *o*C8 chlorine.[20,21] A similar Raman spectrum was reported in ref 2, but the authors assigned it to a pure *Pnma* $NaCl_3$ phase.[2] Raman spectra taken from the samples in DAC #2 (Figure S8a), DAC #3 (Figure S8b), and DACs #4 and #5 (Figure S8c) give evidence of chemical reactions after heating, but we did not analyze them in detail because of the insufficient resolution of individual Raman bands.

3.3. Unraveling the Bonding Complexity of Polyhalogen Anions: Geometrical Similar but Different Infinite Linear Polyhalogen $[X]_\infty^{n-}$ Chains in *c*P8-NaX_3 vs *h*P18-Na_4X_5

Experimental structural data and theoretical calculations provide a basis for discussing crystal chemistry and the nature of chemical bonding in the novel alkali halides. The discrete trichloride anions $[Cl_3]^-$ in the structure of *h*P24-KCl_3 were found to be linear and symmetric (at 41 GPa, the intramolecular Cl1−Cl2 distances are of 2.301(3) Å, while the shortest intermolecular ones are of 2.800(5) Å (Figure S1b)). The $[Cl_3]^-$ anion in *h*P24-KCl_3 is an example of 22-valence electron systems, which are well known in inorganic chemistry[22−25] (XeF_2 and trihalide anions being among them). As several so far known trichloride $[Cl_3]^-$ anions are asymmetric,[22,26] the $[Cl_3]^-$ anion in *h*P24-KCl_3 provides the first example of a symmetric trichloride anion, similar to the symmetric $[Br_3]^-$ and $[I_3]^-$ known at ambient pressure.[22,27] This agrees with the empirical rule of high-pressure crystal chemistry—elements behave at HP like the elements below them in the periodic table at lower pressure.[28]

The *c*P8-AX_3 (A = Na or K, X = Cl or Br) and *h*P18-Na_4X_5 phases also contain polyhalogen anions, but of a different type, infinite linear chains $[Cl]_\infty^{n-}$ and $[Br]_\infty^{n-}$, hitherto unknown for any polyhalides at ambient condition.[22] In the *c*P8-AX_3 compounds, Cl−Cl and Br−Br distances depend on the cation. For example, according to the experimental data, at 50 GPa, Cl−Cl distances in *c*P8-$NaCl_3$ and *c*P8-KCl_3 are of 2.3535(2) and 2.4097(6) Å, respectively. This gives a difference of 0.056(1) Å. At the same pressure, in ionic high-pressure sodium and potassium chlorides, B2-NaCl and B2-KCl, they are of 2.91 and 3.04 Å, respectively, with a difference twice larger.[29,30] In sodium and potassium compounds, such as NaN_3/KN_3, NaC_2/KC_2, and NaO_2/KO_2, featuring molecular anions with strong covalent bonds (N_3^-, C_2^-, and O_2^-), the intramolecular distances are almost similar[31−33] (1.177 and 1.183 Å in N_3^- at ambient pressure, for instance[32]). Thus, the common crystal chemical analysis suggests that in *c*P8-AX_3 compounds, there is a covalent interaction between halogen atoms in infinite chains but much weaker than in molecular anions.

Comparing halogen−halogen distances in the $[Cl]_\infty^{n-}$ and $[Br]_\infty^{n-}$ chains in pairs *c*P8-$NaCl_3$ vs *h*P18-Na_4Cl_5 and *c*P8-$NaBr_3$ vs *h*P18-Na_4Br_5, one can see that in each pair, the difference is of about 0.06 Å (~2.38 vs ~2.44 Å and ~2.53 vs ~2.60 Å in the corresponding chlorides and bromides at 40 GPa). Such a dissimilarity in the separation of halogen atoms in chains of different kind may mean an appreciable variation of formal charges if there is a correlation similar to that found for pernitrides, in which the charge of N_2^{n-} anions varies by one electron unit if its length changes by ~0.05 Å.[31]

In order to further analyze the chemical bonding in $[Cl]_\infty^{n-}$ and $[Br]_\infty^{n-}$ polyhalogen anions, we performed DFT calculations of total and projected electron densities of states (TDOS and PDOS), the electron localization function (ELF), partial charge density across Fermi energy (E_f), the crystal orbital Hamilton population (COHP),[34] and the crystal orbital bond index (COBI),[35] as well as the integrated values of the latter two (ICOHP and ICOBI) (see Figures 4, S9, and S10 for $[Cl]_\infty^{n-}$ and Figure S11 for $[Br]_\infty^{n-}$).

The ELFs confirm that $[Cl]_\infty^{n-}$ and $[Br]_\infty^{n-}$ are conjugated 1D electronic systems forming polyanions (Figures 4 and S11a,b). There are, however, obvious differences in the ELFs of polyanions in *c*P8-NaX_3 trichlorides and *h*P18-Na_4X_5: in the *c*P8-NaX_3 compounds, the electron distribution in the pairs of halogen atoms has a shape of hourglass (Figures 4a and S11a), whereas in *h*P18-Na_4X_5, the electron distribution around each atom is mirror symmetric (Figures 4b and S11b). Both the Löwdin and Bader charges of halogen atoms in the chains of *c*P8-NaX_3 and *h*P18-Na_4X_5 compounds are different (Table S12). The analysis of ICOBI and −ICOHP confirms the existence of chemical bonds between halogen atoms in polyanion chains. The bonding character is intermediate between ionic (ICOBI = 0) and covalent (ICOBI = 1): for *c*P8-$NaCl_3$ at 50 GPa, ICOBI = 0.285, and for *h*P18-Na_4Cl_5, ICOBI = 0.197 (Table S13). Thus, both qualitative crystal-chemical analysis and quantitative data based on our DFT calculations lead to the conclusion that despite geometrical similarities, $[X]_\infty^{n-}$ chains in the *c*P8-NaX_3 and in the *h*P18-Na_4X_5 compounds are different halogen polyanions. Nevertheless, there are common features in the chemical bonding and electron properties of these different $[X]_\infty^{n-}$ chains. The

https://doi.org/10.1021/jacsau.3c00090
JACS Au 2023, 3, 1634−1641

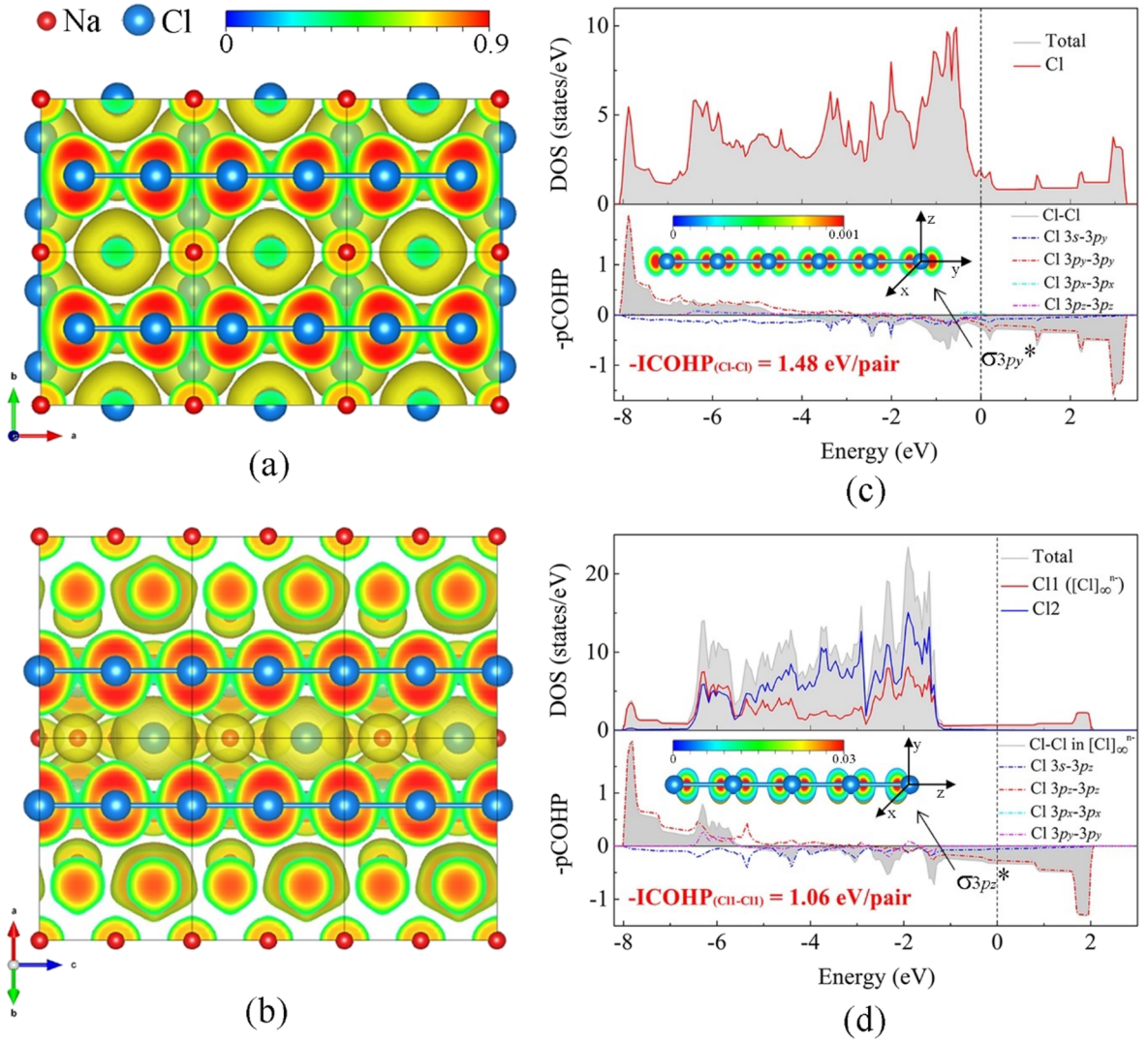

Figure 4. Calculated properties of *cP*8-$NaCl_3$ and *hP*18-Na_4Cl_5 at 50 GPa. (a) Electron localization function (ELF) calculated in the (001) plane for *cP*8-$NaCl_3$ and (b) in the (110) plane for *hP*18-Na_4Cl_5. The isosurface value is set as 0.3. Na and Cl atoms are shown in red and blue colors, respectively. Calculated TDOS and PDOS curves for (c) *cP*8-$NaCl_3$ and (d) *hP*18-Na_4Cl_5 along with the −pCOHP and −ICOHP for the Cl−Cl bond in the linear $[Cl]_\infty^{n-}$ chains. The vertical dashed line indicates the Fermi energy. The insets in panels (c) and (d) show the partial charge density distributions around the Fermi level (-1 eV < $E - E_F$ < 0 eV), which indicate the occupation of σ_{3p}* antibonding orbitals in *cP*8-$NaCl_3$ (σ_{3py}*) and *hP*18-Na_4Cl_5 (σ_{3pz}*).

analysis of the −pCOHP curves (Figure 4c,d) shows the occupation of the antibonding orbitals (both π* and σ*) by halogens' electrons in both *cP*8-$NaCl_3$ (Figure 4c) and *hP*18-Na_4Cl_5 (Figure 4d). These delocalized electrons contribute to the conduction bands making a σ-conjugated system in these materials metallic (see the inserts in Figures 4c,d and S9). In contrast, the $[Cl_3]^-$ ion in *hP*24-KCl_3, which is isoelectronic to XeF_2 with the 4-electron 3-center (4e−3c) hypervalent bonding system,[23−25] is obviously non-metallic (Figure S12). In addition, the −pCOHP curves explain the difference in the ELFs of *cP*8-NaX_3 and *hP*18-Na_4X_5. The two 3p−π interactions (Cl $3p_x$−$3p_x$ and Cl $3p_y$−$3p_y$) in *hP*18-Na_4Cl_5 are similar, so that the corresponding curves in Figure 4d coincide (see also Figure S10b for details). The −pCOHP curves for Cl $3p_x$−$3p_x$ and Cl $3p_z$−$3p_z$ in *cP*8-$NaCl_3$ are different (Figures 4c and S10a) which implies a tilting of the two Cl 3p orbitals in the *xz* plane for *cP*8-$NaCl_3$.

3.4. Unusually Short Contacts between Sodium Cations in Na_4Cl_5 and Na_4Br_5

The interactions between A and X in *hP*24-KCl_3 and *cP*8-AX_3 compounds are ionic since the interatomic A−X distances and Löwdin/Bader charges are similar to those in the corresponding B2-AX salts. That is also confirmed by the analysis of ICOBI values (for example, for *cP*8-$NaCl_3$, the ICOBI of the Na−Cl bond is equal to 0.047, which is comparable to the value for B2-NaCl of 0.057, Tables S12 and S13). For the *hP*18-Na_4X_5 compounds, the analysis of the Löwdin/Bader charges (Table S12) and ICOBI (Table S13) also points out that both structurally distinct Na atoms are in an ionic state. One of the sodium atoms (Na2 in Figure 1c), located in the first coordination sphere of $[X]_\infty^{n-}$ ions in *hP*18-Na_4X_5, is at the distance characteristic for ionic contacts. The second type of Na atoms (see Na1 in Figure 1c) is surrounded by six halogen atoms forming octahedra with a short cation−anion distance (2.351(2) Å in *hP*18-Na_4Cl_5 at 50 GPa from experimental data). These Na1 atoms form chains with very

https://doi.org/10.1021/jacsau.3c00090
JACS Au 2023, 3, 1634−1641

short interatomic contacts (2.3879(9) Å in $hP18$-Na_4Cl_5 at 50 GPa, see Figure 1b). Distances between Na1 atoms in the chains are shorter than in pure metallic Na at the same pressure (2.617 Å at 50 GPa, see Figure 5). Short interatomic contacts result in higher atomic density (for example, from DFT calculations at 50 GPa, the volume per atom of 12.55 $Å^3$ for $hP18$-Na_4Cl_5 is smaller than that of 12.77 $Å^3$ for $cP8$-$NaCl_3$; see Figure S3c,d). According to our DFT calculations, there is no orbital overlapping between Na1 atoms in the chains, or any contribution of sodium's electrons at the Fermi level (Figure S9b), as well as there are no signs that these may be electrides. Thus, our finding suggests that HP can drive contacts between cations (particularly Na^+) much closer than previously known (Figure 5).

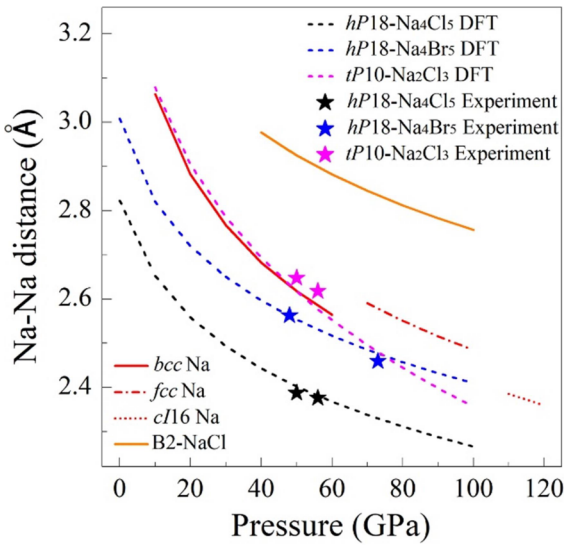

Figure 5. Pressure dependences of the shortest Na−Na distances in different allotropes of sodium[36,37] and B2-NaCl,[30] and in $hP18$-Na_4Cl_5, $hP18$-Na_4Br_5, and $tP10$-Na_2Cl_3.

3.5. Electronic Structure of $tP10$-Na_2Cl_3

The crystal chemistry of $tP10$-Na_2Cl_3 is obviously different from that of the $cP8$-$NaCl_3$ and $hP18$-Na_4Cl_5 phases—its structure does not possess polychlorine anions (Figure S13a). The shortest Na−Cl contacts are quite short (2.425(3) vs 2.52 Å in B2-NaCl[30] at 50 GPa), indicating that chemical bonds are not simple ionic and/or formal charges of Cl ions are smaller than 1 (in absolute value), similarly to those in FeO_2.[38] Our calculations show that Cl atoms in $tP10$-Na_2Cl_3 are not chemically connected with each other and exist as Cl ions with partially occupied p orbitals (Figure S13b).

4. CONCLUSIONS

To summarize, we experimentally studied chemical reactions in the four systems, Na−Cl, Na−Br, K−Cl, and K−Br, at HP and HT. SCXRD analysis revealed AX_3 compounds in all of the studied systems (isostructural $cP8$ $NaCl_3$, $NaBr_3$, KCl_3, and KBr_3, and $hP24$-KCl_3). Three previously unpredicted novel phases were synthesized in the Na−Cl ($tP10$-Na_2Cl_3 and $hP18$-Na_4Cl_5 at 50 and 56 GPa) and Na−Br ($hP18$-Na_4Br_5 at 48 and 73 GPa) systems. On the basis of the structural data and the results of ab initio calculations, we have characterized the chemical bonding of polyhalogen anions and chains and have found that infinite linear halogen chains, $[Cl]_\infty^{n-}$ and $[Br]_\infty^{n-}$, in $hP18$-Na_4Cl_5 and $hP18$-Na_4Br_5 are different from those in sodium and potassium tribromides, $cP8$-$NaCl_3$ and $cP8$-$NaBr_3$. These results give a new insight into the chemistry of polyhalides.

■ ASSOCIATED CONTENT

Data Availability Statement

CSD 2224055, CSD 2224057, and CSD 2224059 contain the supplementary crystallographic data for the novel compounds presented. These data can be obtained free of charge from The Cambridge Crystallographic Data Centre via www.ccdc.cam.ac.uk/data_request/cif.

Supporting Information

The Supporting Information is available free of charge at https://pubs.acs.org/doi/10.1021/jacsau.3c00090.

Supplementary methods, SCXRD measurements and crystallographic details, and equation of states of all synthesized compounds, stability analyses, Raman spectra, Löwdin and Bader charge, electronic structures, and COHP and COBI analyses (PDF)

■ AUTHOR INFORMATION

Corresponding Author

Yuqing Yin − *Material Physics and Technology at Extreme Conditions, Laboratory of Crystallography, University of Bayreuth, Bayreuth 95440, Germany; State Key Laboratory of Crystal Materials, Shandong University, Jinan 250100, China;* orcid.org/0000-0001-8861-8443; Email: Yuqing.Yin@uni-bayreuth.de

Authors

Alena Aslandukova − *Bayerisches Geoinstitut, University of Bayreuth, Bayreuth 95440, Germany*

Nityasagar Jena − *Department of Physics, Chemistry and Biology (IFM), Linköping University, Linköping SE-581 83, Sweden*

Florian Trybel − *Department of Physics, Chemistry and Biology (IFM), Linköping University, Linköping SE-581 83, Sweden*

Igor A. Abrikosov − *Department of Physics, Chemistry and Biology (IFM), Linköping University, Linköping SE-581 83, Sweden*

Bjoern Winkler − *Institute für Geowissenschaften, Frankfurt University, Frankfurt am Main DE-60438, Germany;* orcid.org/0000-0001-8029-478X

Saiana Khandarkhaeva − *Bayerisches Geoinstitut, University of Bayreuth, Bayreuth 95440, Germany;* orcid.org/0000-0001-7345-6066

Timofey Fedotenko − *Photon Science, Deutsches Elektronen-Synchrotron DESY, 22607 Hamburg, Germany*

Elena Bykova − *Bayerisches Geoinstitut, University of Bayreuth, Bayreuth 95440, Germany; Earth and Planets Laboratory, Carnegie Institution for Science, Washington, District of Columbia 20015, United States;* orcid.org/0000-0001-8652-024X

Dominique Laniel − *Centre for Science at Extreme Conditions and School of Physics and Astronomy, University of Edinburgh, Edinburgh EH9 3FD, U.K.*

Maxim Bykov − *Institute of Inorganic Chemistry, University of Cologne, Cologne 50939, Germany*

Andrey Aslandukov − *Material Physics and Technology at Extreme Conditions, Laboratory of Crystallography and Bayerisches Geoinstitut, University of Bayreuth, Bayreuth 95440, Germany;* orcid.org/0000-0003-0988-6066
Fariia I. Akbar − *Material Physics and Technology at Extreme Conditions, Laboratory of Crystallography and Bayerisches Geoinstitut, University of Bayreuth, Bayreuth 95440, Germany*
Konstantin Glazyrin − *Photon Science, Deutsches Elektronen-Synchrotron DESY, 22607 Hamburg, Germany*
Gaston Garbarino − *European Synchrotron Radiation Facility, Grenoble Cedex F-38043, France*
Carlotta Giacobbe − *European Synchrotron Radiation Facility, Grenoble Cedex F-38043, France*
Eleanor L. Bright − *European Synchrotron Radiation Facility, Grenoble Cedex F-38043, France*
Zhitai Jia − *State Key Laboratory of Crystal Materials, Shandong University, Jinan 250100, China;* orcid.org/0000-0002-7534-8082
Leonid Dubrovinsky − *Bayerisches Geoinstitut, University of Bayreuth, Bayreuth 95440, Germany*
Natalia Dubrovinskaia − *Material Physics and Technology at Extreme Conditions, Laboratory of Crystallography, University of Bayreuth, Bayreuth 95440, Germany; Department of Physics, Chemistry and Biology (IFM), Linköping University, Linköping SE-581 83, Sweden*

Complete contact information is available at: https://pubs.acs.org/10.1021/jacsau.3c00090

Author Contributions

L.D., N.D., and Y.Y. designed the study. L.D. and N.D. supervised the research. Y.Y., S.K., T.F., E.B., D.L., M.B., A.A., F.I.A., L.D., K.G., G.G., C.G., and E.L.B. conducted the experiments. Theoretical calculations were performed by Y.Y., A.A., B.W., N.J., F.T., and I.A.A. Y.Y., L.D., and N.D. wrote the paper with contributions from all authors. A.A., D.L., A.A., and Z.J. reviewed and edited the draft. All authors have given approval to the final version of the manuscript.

Notes

The authors declare no competing financial interest.

■ ACKNOWLEDGMENTS

The authors acknowledge the Deutsches Elektronen-Synchrotron (DESY, PETRA III) and the European Synchrotron Radiation Facility (ESRF) for provision of beamtime at the P02.2, and ID11 and ID27 beamlines, respectively. Y.Y. acknowledges the financial support provided by the China Scholarship Council (CSC) during her visit to the University of Bayreuth. N.D. and L.D. thank the Federal Ministry of Education and Research, Germany (BMBF, grant no. 05K19WC1), and the Deutsche Forschungsgemeinschaft (DFG; projects DU 954-11/1, DU 393-9/2, and DU 393-13/1) for financial support. N.D. also thanks the Swedish Government Strategic Research Area in Materials Science on Functional Materials at Linköping University (Faculty grant SFO-Mat-LiU no. 2009 00971). M.B. acknowledges the support of Deutsche Forschungsgemeinschaft (DFG Emmy-Noether project BY112/2-1). D.L. thanks the UKRI Future Leaders Fellowship (MR/V025724/1) for financial support. N.J., F.T., and I.A.A. acknowledge support by the Knut and Alice Wallenberg Foundation (Wallenberg Scholar grant no. KAW-2018.0194). Support from the Swedish Research Council (VR) grant no. 2019-05600 and the Swedish Government Strategic Research Areas in Materials Science on Functional Materials at Linköping University (Faculty grant SFO-Mat-LiU no. 2009 00971) is gratefully acknowledged. DFT calculations were enabled by resources provided by the National Academic Infrastructure for Supercomputing in Sweden (NAISS) at National Supercomputer Center partially funded by the Swedish Research Council through grant agreement no. 2022-06725.

■ REFERENCES

(1) Miao, M. S.; Sun, Y. H.; Zurek, E.; Lin, H. Q. Chemistry under high pressure. *Nat. Rev. Chem.* **2020**, *4*, 508−527.
(2) Zhang, W.; Oganov, A. R.; Goncharov, A. F.; Zhu, Q.; Boulfelfel, S. E.; Lyakhov, A. O.; Stavrou, E.; Somayazulu, M.; Prakapenka, V. B.; Konopkova, Z. Unexpected stable stoichiometries of sodium chlorides. *Science* **2013**, *342*, 1502−1505.
(3) Saleh, G.; Oganov, A. R. Alkali subhalides: high-pressure stability and interplay between metallic and ionic bonds. *Phys. Chem. Chem. Phys.* **2016**, *18*, 2840−2849.
(4) Botana, J.; Brgoch, J.; Hou, C.; Miao, M. Iodine Anions beyond -1: Formation of LinI (n = 2-5) and Its Interaction with Quasiatoms. *Inorg. Chem.* **2016**, *55*, 9377−9382.
(5) Miao, M. S. Caesium in high oxidation states and as a p-block element. *Nat. Chem.* **2013**, *5*, 846−852.
(6) Zhu, Q.; Oganov, A. R.; Zeng, Q. Formation of stoichiometric CsFn compounds. *Sci. Rep.* **2015**, *5*, 7875.
(7) Zhang, W.; Oganov, A. R.; Zhu, Q.; Lobanov, S. S.; Stavrou, E.; Goncharov, A. F. Stability of numerous novel potassium chlorides at high pressure. *Sci. Rep.* **2016**, *6*, 26265.
(8) Patel, N. N.; Verma, A. K.; Mishra, A. K.; Sunder, M.; Sharma, S. M. The synthesis of unconventional stoichiometric compounds in the K-Br system at high pressures. *Phys. Chem. Chem. Phys.* **2017**, *19*, 7996−8007.
(9) Patel, N. N.; Sunder, M.; Garg, A. B.; Poswal, H. K. Pressure-induced polymorphism in hypervalent CsI3. *Phys. Rev. B* **2017**, *96*, No. 174114.
(10) Poreba, T.; Racioppi, S.; Garbarino, G.; Morgenroth, W.; Mezouar, M. Investigating the Structural Symmetrization of CsI3 at High Pressures through Combined X-ray Diffraction Experiments and Theoretical Analysis. *Inorg. Chem.* **2022**, *61*, 10977.
(11) Dubrovinskaia, N.; Dubrovinsky, L. Crystallography taken to the extreme. *Phys. Scr.* **2018**, *93*, No. 062501.
(12) Aslandukov, A.; Aslandukov, M.; Dubrovinskaia, N.; Dubrovinsky, L. Domain Auto Finder (DAFi) program: the analysis of single-crystal X-ray diffraction data from polycrystalline samples. *J. Appl. Crystallogr.* **2022**, *55*, 1383−1391.
(13) Dubrovinsky, L.; Khandarkhaeva, S.; Fedotenko, T.; Laniel, D.; Bykov, M.; Giacobbe, C.; Lawrence Bright, E.; Sedmak, P.; Chariton, S.; Prakapenka, V.; Ponomareva, A. V.; Smirnova, E. A.; Belov, M. P.; Tasnádi, F.; Shulumba, N.; Trybel, F.; Abrikosov, I. A.; Dubrovinskaia, N. Materials synthesis at terapascal static pressures. *Nature* **2022**, *605*, 274−278.
(14) Bykov, M.; Chariton, S.; Bykova, E.; Khandarkhaeva, S.; Fedotenko, T.; Ponomareva, A. V.; Tidholm, J.; Tasnadi, F.; Abrikosov, I. A.; Sedmak, P.; Prakapenka, V.; Hanfland, M.; Liermann, H. P.; Mahmood, M.; Goncharov, A. F.; Dubrovinskaia, N.; Dubrovinsky, L. High-Pressure Synthesis of Metal-Inorganic Frameworks Hf4 N20 N2 , WN8 N2 , and Os5 N28 3 N2 with Polymeric Nitrogen Linkers. *Angew. Chem., Int. Ed. Engl.* **2020**, *59*, 10321−10326.
(15) Pravica, M.; Sneed, D.; Wang, Y.; Smith, Q.; Subrahmanyam, G. Carbon tetrachloride under extreme conditions. *J. Chem. Phys.* **2014**, *140*, 194503.

(16) Pravica, M.; Sneed, D.; Smith, Q.; Bai, L. High pressure X-ray photochemical studies of carbon tetrachloride: Cl2 production and segregation. *Chem. Phys. Lett.* **2013**, *590*, 74−76.
(17) Fedotenko, T. In *personal communication*, 2022.
(18) Aprilis, G.; Kantor, I.; Kupenko, I.; Cerantola, V.; Pakhomova, A.; Collings, I. E.; Torchio, R.; Fedotenko, T.; Chariton, S.; Bykov, M.; Bykova, E.; Koemets, E.; Vasiukov, D. M.; McCammon, C.; Dubrovinsky, L.; Dubrovinskaia, N. Comparative study of the influence of pulsed and continuous wave laser heating on the mobilization of carbon and its chemical reaction with iron in a diamond anvil cell. *J. Appl. Phys.* **2019**, *125*, No. 095901.
(19) Hamilton, W. C. Significance tests on the crystallographic R factor. *Acta Crystallogr.* **1965**, *18*, 502−510.
(20) Johannsen, P. G.; Holzapfel, W. B. Effect of pressure on Raman spectra of solid chlorine. *J. Phys. C: Solid State Phys.* **1983**, *16*, L1177−L1179.
(21) Dalladay-Simpson, P.; Binns, J.; Pena-Alvarez, M.; Donnelly, M. E.; Greenberg, E.; Prakapenka, V.; Chen, X. J.; Gregoryanz, E.; Howie, R. T. Band gap closure, incommensurability and molecular dissociation of dense chlorine. *Nat. Commun.* **2019**, *10*, 1134.
(22) Sonnenberg, K.; Mann, L.; Redeker, F. A.; Schmidt, B.; Riedel, S. Polyhalogen and Polyinterhalogen Anions from Fluorine to Iodine. *Angew. Chem., Int. Ed. Engl.* **2020**, *59*, 5464−5493.
(23) Braida, B.; Hiberty, P. C. The essential role of charge-shift bonding in hypervalent prototype XeF(2). *Nat. Chem.* **2013**, *5*, 417−422.
(24) Sun, Z.; Moore, K. B., 3rd; Hill, J. G.; Peterson, K. A.; Schaefer, H. F., 3rd; Hoffmann, R. Alkali-Metal Trihalides: M(+)X3(−) Ion Pair or MX-X2 Complex? *J. Phys. Chem. B* **2018**, *122*, 3339−3353.
(25) Munzarova, M. L.; Hoffmann, R. Electron-rich three-center bonding: role of s,p interactions across the p-block. *J. Am. Chem. Soc.* **2002**, *124*, 4787−4795.
(26) Keil, H.; Sonnenberg, K.; Muller, C.; Herbst-Irmer, R.; Beckers, H.; Riedel, S.; Stalke, D. Insights into the Topology and the Formation of a Genuine ppsigma Bond: Experimental and Computed Electron Densities in Monoanionic Trichlorine [Cl3]. *Angew. Chem., Int. Ed. Engl.* **2021**, *60*, 2569−2573.
(27) Pichierri, F. Structure and bonding in polybromide anions Br−(Br2)n (n=1−6). *Chem. Phys. Lett.* **2011**, *515*, 116−121.
(28) Prewitt, C. T.; Downs, R. T. High-pressure crystal chemistry. *Rev. Mineral.* **1998**, *37*, 284−318.
(29) Dewaele, A.; Belonoshko, A. B.; Garbarino, G.; Occelli, F.; Bouvier, P.; Hanfland, M.; Mezouar, M. High-pressure−high-temperature equation of state of KCl and KBr. *Phys. Rev. B: Condens. Matter Mater. Phys.* **2012**, *85*, No. 214105.
(30) Sata, N.; Shen, G.; Rivers, M. L.; Sutton, S. R. Pressure-volume equation of state of the high-pressureB2phase of NaCl. *Phys. Rev. B: Condens. Matter Mater. Phys.* **2002**, *65*, No. 104114.
(31) Laniel, D.; Winkler, B.; Fedotenko, T.; Aslandukova, A.; Aslandukov, A.; Vogel, S.; Meier, T.; Bykov, M.; Chariton, S.; Glazyrin, K.; Milman, V.; Prakapenka, V.; Schnick, W.; Dubrovinsky, L.; Dubrovinskaia, N. High-pressure Na3(N2)4, Ca3(N2)4, Sr3(N2)4, and Ba(N2)3 featuring nitrogen dimers with noninteger charges and anion-driven metallicity. *Phys. Rev. Mater.* **2022**, *6*, No. 023402.
(32) Eremets, M. I.; Popov, M. Y.; Trojan, I. A.; Denisov, V. N.; Boehler, R.; Hemley, R. J. Polymerization of nitrogen in sodium azide. *J. Chem. Phys.* **2004**, *120*, 10618−10623.
(33) Laniel, D.; Trybel, F.; Yin, Y.; Fedotenko, T.; Khandarkhaeva, S.; Aslandukov, A.; Aprilis, G.; Abrikosov, A. I.; Bin Masood, T.; Giacobbe, C. J. N. C. Aromatic hexazine [N6] 4− anion featured in the complex structure of the high-pressure potassium nitrogen compound K9N56. *Nat. Chem.* **2023**, *15*, 641−646.
(34) Dronskowski, R.; Bloechl, P. E. Crystal orbital Hamilton populations (COHP): energy-resolved visualization of chemical bonding in solids based on density-functional calculations. *J. Phys. Chem.* **1993**, *97*, 8617−8624.
(35) Müller, P. C.; Ertural, C.; Hempelmann, J.; Dronskowski, R. Crystal Orbital Bond Index: Covalent Bond Orders in Solids. *J. Phys. Chem. C* **2021**, *125*, 7959−7970.
(36) Gregoryanz, E.; Lundegaard, L. F.; McMahon, M. I.; Guillaume, C.; Nelmes, R. J.; Mezouar, M. Structural diversity of sodium. *Science* **2008**, *320*, 1054−1057.
(37) Ma, Y.; Eremets, M.; Oganov, A. R.; Xie, Y.; Trojan, I.; Medvedev, S.; Lyakhov, A. O.; Valle, M.; Prakapenka, V. Transparent dense sodium. *Nature* **2009**, *458*, 182−185.
(38) Koemets, E.; Leonov, I.; Bykov, M.; Bykova, E.; Chariton, S.; Aprilis, G.; Fedotenko, T.; Clement, S.; Rouquette, J.; Haines, J.; Cerantola, V.; Glazyrin, K.; McCammon, C.; Prakapenka, V. B.; Hanfland, M.; Liermann, H. P.; Svitlyk, V.; Torchio, R.; Rosa, A. D.; Irifune, T.; Ponomareva, A. V.; Abrikosov, I. A.; Dubrovinskaia, N.; Dubrovinsky, L. Revealing the Complex Nature of Bonding in the Binary High-Pressure Compound FeO2. *Phys. Rev. Lett.* **2021**, *126*, No. 106001.

https://doi.org/10.1021/jacsau.3c00090
JACS Au 2023, 3, 1634−1641